Landscape genetics of the copal tree, Bursera cuneata (Burseraceae): The key role of the Tropical Dry Forest in shaping connectivity at the regional scale

Yessica Rico
yessica.rico@inecol.mx
Instituto de Ecologia
Marisol Zurita-Solis
Instituto de Ecologia https://orcid.org/0000-0002-9026-6552
Bode Olukolu
University of Tennessee https://orcid.org/0000-0003-4143-8909

Article

Keywords: Burseraceae, functional connectivity, gene flow, SNPs, tropical dry forest, Mexico

Posted Date: November 6th, 2025

DOI: https://doi.org/10.21203/rs.3.rs-7724981/v1

Additional Declarations: There is no duality of interest

Version of Record: A version of this preprint was published at Heredity on June 24th, 2026. See the published version at https://doi.org/10.1038/s41437-026-00858-1.

Abstract

Land-use changes in tropical dry forests (TDF) have rapidly reduced native vegetation, disrupting gene flow dynamics of tree species. Bursera cuneata is a co-dominant TDF tree in central Mexico, is threatened by habitat loss and overexploitation. We investigated landscape drivers of functional connectivity of B. cuneata across scales to inform species conservation efforts. We genotyped 227 B. cuneata individuals from 33 populations across five hydrological basins at 10,499 single-nucleotide polymorphism (SNP) loci. We examined spatial patterns of genetic structure among hydrological basins and the landscape drivers of gene flow. We applied gravity models that incorporated at-site (slope and east aspect) and between-site (terrain roughness, habitat suitability, and habitat cover) factors influencing B. cuneata gene flow. Clustering analyses showed genetic structure among basins, with the highest differentiation for Balsas (BAL) and Mexico (MEX). Gravity models revealed that functional connectivity is a scale-dependent process. Specifically, terrain roughness was the primary factor of connectivity at finer scales (1,000–3,000 m), while the TDF became the main driver at regional scales (>4,000 m). We recommend protecting and prioritizing crucial TDF remnants to maintain large-scale gene flow by integrating urban natural parks as important links to prevent genetic isolation between urban and rural populations.

Introduction

The Tropical Dry Forest (TDF) is a critically important ecosystem, representing 42% of the world's tropical forests, hosting a diverse group of endemic plants and animals (Murphy and Lugo 1986; Rzedowski 1991; Blackie et al. 2014; Mesa-Sierra et al. 2022b). Its ecological significance is driven by its pronounced seasonal variability, diverse topography, and soil properties (Powers et al. 2018; Méndez-Toribio et al., 2017; Quisehuatl-Medina et al., 2023). These factors not only sustain high species richness but also play a vital role in global carbon sequestration (Mesa-Sierra et al. 2022a). In Mexico, despite being one of the most extensive ecosystems, it is highly threatened, having lost approximately 75% of its original area (Trejo and Dirzo 2000; Rzedowski 2006). The remaining TDFs are mostly transformed into secondary forests and scattered within anthropized landscapes of agriculture, cattle pastures, and urban developments (Bezaury-Creel 2010). Habitat loss and increasing isolation threaten plant communities by affecting essential ecological processes, such as limiting propagule dispersal and gene flow among populations (Auffret *et al*., 2017).

Among the flora of the Mexican TDF are trees of the genus *Bursera* (Rzedowski and Kruse 1979; Rzedowski and Gevara-Féfer 1992; Espinosa et al. 2006; Steinmann 2021), whose global center of species diversity and endemicity is the western Balsas Basin (Becerra 2005; Becerra and Venable 2008). The *Bursera* genus consists of aromatic trees and shrub species (~ 100) with resinous leaves and trunks (Rzedowski and Medina-Lemos, 2023). *Bursera* has held cultural importance since pre-Colombian times, providing aromatic resins for religious and medicinal purposes, which continues to date (Montúfar-López, 2016). Habitat loss poses the most critical threat to the survival of *Bursera* species. Recent assessments reveal that 67% of *Bursera* taxa are listed as threatened on the IUCN Red List, primarily due to ongoing TDF loss and degradation (Fuentes *et al*., 2019).

Landscape genetics, which explicitly integrates spatial variables with population genetic data (Holderegger *et al*., 2010; Cruzan and Hendrickson, 2020), has become a key tool for quantifying functional connectivity (i.e, gene flow). This approach directly informs conservation planning in anthropized landscapes (Balzotti *et al*., 2020), such as the TDF, where only a small portion is protected under natural parks (Mesa-Sierra *et al*., 2022b). For plants, functional connectivity refers to the effective dispersal of seeds and pollen across the landscape matrix mediated by dispersal vectors and local factors influencing establishment (Auffret *et al*., 2017). Thus, connectivity is shaped by drivers operating at multiple spatial scales. At a fine scale, topographic features, such as slope aspect and steepness, influence microclimate conditions (e.g., humidity and temperature), which affect propagule establishment (Méndez-Toribio et al., 2014, 2016). These heterogeneous microhabitats found in steep rocky areas can be crucial for specialized species (Eisenlohr et al., 2013). At a broader, regional scale, functional connectivity is driven by land cover composition, remnant forest patches, and transitional habitats that facilitate vector movement (Dileo et al., 2014; Cristóbal-Pérez et al., 2021). Therefore, to effectively evaluate the conservation status of vulnerable tree species in the TDF, it is essential to assess how these multi-scale landscape drivers influence functional connectivity (Cruzan and Hendrickson, 2020; Hoban et al., 2021).

Large areas of the TDF along the Trans-Mexican Volcanic Belt (TMVB), particularly in the states of Michoacán, México State, Guanajuato, Querétaro, and Morelos, have been dramatically lost to agricultural expansion, livestock grazing, and mining (Hernández-Oria, 2007). This region has also undergone intensive urban and industrial development due to commercial growth. Among the affected species is *Bursera cuneata*, a dominant TDF tree (Cué-Bär *et al*., 2006), whose wood is used for handicrafts in Michoacán, and which has experienced significant local population declines (Rzedowski and Guevara-Féfer, 1992; Luft-Dávalos and Álvarez Icaza, 2009). *Bursera cuneata* shows a patchy distribution across five environmentally diverse hydrological basins within central Mexico's Trans-Mexican Volcanic Belt (Rzedowski and Guevara-Féfer, 1992; Flores-Estrella *et al*., 2007; Caballero *et al*., 2010). These basins, Lerma-Chapala (CHA; 500- 2,000 m.a.s.l.), Pátzcuaro (PTZ; 2,000-2,050 m. a.s.l.), Cuitzeo (CTZ; 1,800- 3,400 m.a.s.l.), México (MEX; 2,240 m.a.s.l.), and Balsas (BAL; 0- 2,000 m.a.s.l.), display significant environmental and topographic heterogeneity (INEGI, 2021). The species primarily inhabits TDF and transitional zones with Temperate Forest (Israde-Alcántara *et al*., 2005), with the most severe TDF degradation occurring in PTZ, CTZ, and MEX basins (Mesa-Sierra *et al*., 2022b). In some areas, such as Mexico City, the species occurs in natural areas and parks within the urban metropolis, where it maintains small and isolated remnant populations.

Despite the ecological importance of *Bursera* species, conservation genetic studies remain scarce, and most studies available are on their phylogenetic relationships (e.g. Becerra and Venable, 1999; Becerra, 2003; Weeks and Simpson, 2007; Rosell *et al*., 2010), with a single study on gene flow (Dunphy and Hamrick, 2007). Here, using single-nucleotide polymorphisms (SNPs), we investigated spatial patterns of genetic structure in *B. cuneata* across five hydrological basins, where we expect to find genetic differentiation due to the marked topographic and environmental heterogeneity among basins. Furthermore, we assessed the relative influence of topographic, environmental, and the proportion of habitat composition on functional connectivity across spatial scales. We expected that, at local scales, east aspect and steepness likely influence *Bursera* establishment (Méndez-Toribio et al., 2014), while habitat suitability and the proportion of TDFs drive gene flow at broader scales. Conversely, the proportion of urbanization and agricultural areas may restrict pollinator movement and seed dispersal.

Materials and methods

Study species and sampling

Bursera cuneata is a dioecious tree, up to 10 m tall, with gray or gray-reddish non-exfoliating bark. The inflorescences are open panicles, blooming from April to July. The main seed vectors are birds of the genera *Melanerpes, Icterus,* and *Myiarchus* (Cultid-Medina and Rico 2020). Although coyotes and mice may also disperse the seed. The pollinators in the genus *Bursera* are insects such as Diptera of the genus *Strigoderma* and *Diogmites*, Coleoptera of the genus *Bleparida* and *Chrysoprasis*, and Hymenoptera of the genus *Apis* and *Hypanthidium*, and some lizards *Microlophus* (Rivas-Arancibia et al. 2015; Maya-Elizarrarás et al. 2024).

We randomly collected two to three leaves from juvenile and adult trees along remnant TDF fragments across the five basins between the years 2017 to 2019. We registered the GPS coordinates for each sampled tree. Leaves were preserved in sealable plastic bags with silica gel until their DNA extraction. Our sampling included 33 populations from the five hydrological basins, of which CHA, PTZ, and CTZ were the basins with the highest occurrence of *B. cuneata* (Fig. 1).

DNA extraction and molecular analysis

Approximately 20-30 mg of genomic DNA from each of 350 samples was extracted from dried tissue using the Cetyl Trimethyl Ammonium Bromide (CTAB) protocol with pre-wash steps to eliminate excess polyphenols (Healey et al., 2014). DNA quantification and purity evaluation were obtained using Quant-iT^{TM} PicoGreen ^{TM} dsDNA Assay and NanoDropTM 2000 (Thermo Fisher Scientific), respectively. A total of 25 ng of high molecular weight DNA was sequentially digested with NsiI-HF and NlaIII restriction enzymes. Barcoded adapters were incorporated into genomic fragments following the OmeSeq-qRRS (quantitative reduced representation sequencing) method (Yencho and Olukolu 2022). Following library preparation, the libraries were diluted to 10 nmol/l and sequenced on a single lane of the NovaSeq S4 flow cell system (150-bp paired-end reads).

SNP filtering

The OmeSeq-qRRS raw reads were demultiplexed and quality filtered using the automated pipeline ngsComposer (Kuster et al. 2021; https://github.com/XXXX/). Variant calling and filtering were performed using the GBSapp automated pipeline (https://github.com/XXXX/). Using this pipeline, all individual reads were mapped against the whole-genome assembly of *B. cuneata* (Rico et al. 2022). Only reads with at least a mapping quality of 20 and that area was uniquely mapped (i.e. excludes reads derived from paralogous sequences) were used for variant calling. These variants were subjected to additional filtering to retain only biallelic markers using the R package *vcfR* (Knaus and Grünwald 2017). To assess the neutral genetic structure and genetic diversity, we used variants with a Phred quality level > 30 (indicating high confidence in variant calling) with the R package *hierfstat* (Goudet 2005), and the R package *adegenet* (Jombart and Ahmed 2011).

Loci potentially under selection (outlier loci) were removed to consider loci only under neutral processes. For this, we considered population structure evaluated with the *snmf* function of the R package *LEA* (Frichot and François 2015) and controlling the false discovery rates by adjusting the *P values* with the genomic inflation value (λ), setting the rates at q = 0.05 with the Benjamini-Hochberg algorithm (François et al. 2016). Moreover, we used the R package *pcadapt* v.4.3 (Privé et al. 2020) by selecting the first three components to identify outlier loci (MAF > 0.05). The matching outlier loci detected by LEA and pcadapt were removed from the total SNP dataset for subsequent analyses.

Genetic diversity, structure, and migration rates

We calculated genetic diversity parameters per basin, such as the number of private alleles (A_p), total number of alleles (A), nucleotide diversity (π), observed (H_o) and unbiased expected heterozygosity (uH_e), and fixation index (F_{IS}) using the R package *dartR* (Gruber et al. 2018). We performed an Analysis of Molecular Variance (AMOVA) to evaluate the amount of genetic variance explained among populations, and among the five basins using the R package *adegenet*, and *poppr* (Kamvar et al. 2014). F_{ST} pairwisecomparisons among basins were estimated using *dartR* and *hierfstat*.

To assess genetic structure, we used the R package *adegenet* to perform a Discriminant Analysis of Principal Components (DAPC), which is a robust genetic clustering method free of Linkage disequilibrium (LD), and Hardy-Weinberg (HW) assumptions (Jombart and Ahmed 2011). We designated the five basins as a priori grouping (CHA, PTZ, CTZ, BAL, and MEX) to visualize genetic and spatial structure. We graphically visualized the first two discriminant functions using scatter plots in R. Also, we implemented a sparse non-negative matrix factorization (*snmf*) from *LEA* R package, setting K = 1 to 7 with 100,000 iterations. To choose the optimal *K,* the cross-entropy criterion was used. For this, *LEA* considers the ancestry coefficients, based on the number of ancestral populations (*snmf*), which are related to the number of principal components of the genomic data, and the latent factor mixed models (*lfmm*) (Frichot and François 2015). The individual ancestry coefficients were grouped and averaged per population and plotted in the geographic space using pie charts.

Moreover, spatial patterns of genetic structure were evaluated by performing Moran´s Eigenvector Maps (MEM) in the R package *MEMgene* (Galpern et al. 2014) using individual GPS coordinates and genetic distances. We plotted significant positive or negative Moran Eigenvector maps that contained the largest genetic variation. To evaluate the effects of isolation by distance (IBD) on genetic differentiation, we performed a Mantel test using the population F_{ST}distances against Euclidean distances. Significance was estimated by permuting observations 1,000 times using the R library *vegan v.2.5.7* (Oksanen et al. 2020). Lastly, we estimated the contemporary migration rates of *B. cuneata* across the five basins using *BayesAss v. 3.0.5.7*. (Wilson and Rannala 2003), with 10,000,000 Markov Chain Monte Carlo (MCMC) iterations and 1,000,000 of burning.

Functional connectivity hypotheses

We downloaded the 2017 Land Use/Land Cover images from Sentinel at 10 m resolution (ESRI Living Atlas: https://livingatlas.arcgis.com/landcover/) to obtain one raster using QGIS v. 3.32 for the landscape genetic analysis (see below). That raster was reclassified to include the following covers: 1) Tropical Dry Forest (TDF), 2) Temperate Forest (pine-oak; TF), 3) permanent and temporary agricultural areas including bare soil (Agri), 4) urban cities (Urb), 5) main water bodies (Lake Cuitzeo, Lake Pátzcuaro, Yuriria lagoon). Also, we characterized the topography of the study area by calculating the slope, terrain roughness (the variability of the terrain's surface, indicating the unevenness of the terrain), and east aspect (most collection populations were found on the east-facing hillsides, and eastness was calculated as the sine of the aspect, values ranging from 1 to -1), using a digital elevation model at 10 m resolution from INEGI (https://www.inegi.org.mx/) using the terrain function in the *raster* v.3.5 package (Hijmans 2022).

To include the environment in the landscape genetic analysis, we built a habitat suitability model using Ecological Niche Models (ENM) for *B. cuneata*. We used 405 points: 227 occurrences of *B. cuneata* (samples analyzed in this study, see results), and 117 records downloaded from The Global Biodiversity Information Facility (GBIF; https://www.gbif.org/es/). To clean the data, we used the niche tool box (*NTBOX*) R package (Osorio-Olvera et al. 2020), considering that the specimens with insufficient locality information were discarded. All occurrences were thinned at five kilometers due to a higher density of occurrences than the training data sets. As variable predictors, we used the 19 bioclimatic variables at 30 s from WorldClim (https://www.worldclim.org/data/worldclim21.html). The bioclimatic layers were delimited by five terrestrial ecoregions downloaded from World Wildlife (https://www.worldwildlife.org/publications/terrestrial-ecoregions-of-the-world). The ecoregions were: Bajío dry forests, Central Mexican scrub, Balsas dry forests, Sierra Madre del Sur pine-oak forests, and Trans Mexican Volcanic Belt pine-oak forests.

The 19 variables were tested individually and in a multivariate analysis, discarding correlated variables using R package *adegenet* ($r \geq 0.8$), and using the first two synthetic axes from 250 Principal Components Analysis (PCA) as covariates. Individual occurrences were used to extract values from the 19 bioclimatic layers. To minimize the redundancy variable, Pearson's correlation was used with a threshold of 0.8 using the R package *NTBOX.* Once the uncorrelated variables were obtained and to have a better balance between the number of occurrences and the number of bioclimatic variables, the niche model was built with the 0.7 threshold (Dormann et al. 2012), under the maximum entropy algorithm in *MAXENT* v3.4.1 (Phillips et al. 2017), using in the *KUENM* v.1.1.1 R package (Cobos et al. 2019). Some levels of the model were evaluated by varying regularization multiplier (RM) from 0.5 to 10 every 0.5, and feature classes linear (L), quadratic (Q), hinge (H), product (P), and threshold (T) in five fixed combinations: L, LQ, LQH, LQHP, and LQHPT, which resulted in 85 candidate niche models. The evaluation was made using 10,000 random background points, five percent of training data omission rate, 20 % for bootstrapping to calculate the partial Receiver Operating Characteristic (pROC) with 10,000 iterations. Also, it was considered for the model evaluation, "evaluate" in R, using 20% of the points that were left out during model training. In addition to this, the *dismo* and *Biodiversity* R packages were used to evaluate the Ecoclimatic Index (EI), which represents the climatic suitability of the species under the regional climate (Kriticos et al. 2015; Yoon and Lee 2023). With the same package, the average value of True Skill Statistic (TSS) was calculated, which is the metric used to evaluate the efficiency of machine learning in the species distribution model (Allouche et al. 2006). The best model was selected from the lowest values of the corrected Akaike information criterion (AICc) and the omission rate.

Landscape genetic analysis

To quantify landscape-genetic relationships in *B. cuneata*, we implemented a spatial gravity model using the *GeNetIt* R package (v.0.1-6; Evans and Murphy 2022). This graph-theoretic framework represents populations as nodes, with edges (straight lines) connecting nodes as proxies of gene flow. Edges were weighted by geographic distance and landscape elements derived from the topographic variables, vegetation type covers, and the habitat suitability model. One of the key advantages of gravity models is their ability to incorporate both at-site and between-site landscape characteristics, allowing a simultaneous evaluation of the local and broad-landscape effects on functional connectivity. To test landscape effects on *B. cuneata* gene flow, we developed several hypotheses where tropical dry forest (TDF), temperate forest (TF), agriculture (Agri), urban areas (Urb), terrain roughness (Rough), and suitable habitat areas (Niche) may facilitate or restrict gene flow at the landscape scale, while slope steepness (Slope) and east aspect (Aspect) may influence local establishment. As a null model, we used Euclidean distance (Geo), in which no landscape effects are predicted. Genetic distances between populations were quantified using the Nei estimator (Nei 1978) using *adegenet* R package and with 1-Nei as a measure of gene flow in the gravity models. All landscape variables were standardized to 30 m resolution.

To assess how functional connectivity changes at different scales and capture greater environmental variation (Murphy et al. 2010), we created five buffers of 1,000 m to 5,000 m for each landscape variable based on the movement range of *B. cuneata* dispersers (Cultid-Medina and Rico 2020). Using *GeNetIt* for continuous variables, we calculated each buffer's mean, maximum, and minimum, while for categorical variables, the relative percentage of each landscape cover was estimated. To ensure independence at the nodes when estimating the gravity models, the variables were transformed to natural logarithms to linearize the equation and implement mixed effects models. We tested the correlation between variables ($r \geq 0.7$) to eliminate correlated variables for multivariate gravity models. In addition to univariate models, we built three combined models, which include variable combinations predicted to significantly influence functional connectivity: Model comb1) Geo, TDF, and Niche (functional connectivity depends on environmentally suitable populations and the proportion of TDF between populations); Comb2) Geo, TDF, and TF (functional connectivity depends on the proportion of TDF and TF between populations); and comb3) Geo, TDF, TF, Niche, and Rough (functional connectivity depends on environmentally suitable populations, proportion of TDF and TF forests, and the roughness of the terrain). We tested univariate between-site and at-site models, and combined models using maximum-likelihood (ML), including the null model (Geo), and for each of the five buffer scales. Models with a *P value* > 0.05, ΔAIC < 4 as the cut-off (Akaike 1973; Romero-Báez et al. 2024), and the lowest AIC were selected. Moreover, we calculated the percentage of explained variance (PVE) using the function *fit.gnet* in *GeNetIt* package to compare between models. For the final model, the restricted maximum likelihood (REML) statistics were used, and confidence intervals measured by Cohen's D were estimated to evaluate each variable's relative importance. These also give a positive or negative value for the size effect, indicating the directionality of the model components (Grizzard and Shaw 2017).

Results

Of the 350 individuals sequenced using the OmeSeq-qRRS method, only 227 passed various quality filtering thresholds. Following quality filtering, the data set included 11,731 SNPs with < 30 % of total missing SNPs and < 20 % of missing samples. The analysis of outlier loci in *LEA* suggested that 4,342 loci were potentially under selection (MAF > 0.05) while 3,110 loci were suggested by *pcadapt* (MAF > 0.05). A total of 1,232 loci were shared between the two methods, which were then removed, resulting in a neutral data set of 10,499 neutral biallelic loci used in subsequent analyses.

Genetic diversity, structure, and migration rates

The genetic diversity values obtained were similar among basins, but CTZ basin has the highest value (π = 0.3117), followed by BAL (π = 0.1964), and PTZ (π = 0.1919). In contrast, CHA (π = 0.1787), and MEX (π = 0.1580) showed the lowest values of diversity (Table 1). CHA and BAL basins showed the highest F_{IS} values; BAL showed the highest number of private alleles. The CHA and BAL basins exhibited the highest F_{IS} values, with BAL displaying the highest number of private alleles(Table 1). The AMOVA among populations showed no significant genetic variance explained (1.1 %, F_{ST} = 0.09, P > 0.05). When analyzing the five basins, we observed a significant genetic variance explained among basins of 8.5% (F_{CT} = 0.0095, P < 0.01), although the greatest genetic variation was found within populations (52%, F_{ST} = 0.00086, P < 0.001) (Table 2). The F_{ST} values obtained per basin showed that MEX basin has high F_{ST}values and was the most differentiated basin (Appendix S1).

The *LEA* analysis identified the optimal number of genetic clusters as K = 5 (Appendix S2). The PTZ basin exhibited high admixture with neighboring basins, such as CHA and CTZ, while lower admixture with MEX and BAL. In contrast, BAL and MEX showed higher genetic differentiation from the rest (Fig. 2A). The DAPC showed that BAL was the most separated from the rest, followed by MEX along DA axis 1, while CTZ was separated along the DA axis 2 (Fig. 2B), and the DAPC also showed that CHA was located on DA axis 3 (Fig. 2C). Moreover, CTZ, PTZ, and CHA, showed higher genetic similarity, which is consistent with the results revealed by *LEA*.

The Moran´s Eigenvector Maps (MEM) analysis revealed two significant and positive MEM vectors. The MEM1 (r = 0.0686, P = 0.039) represents the first eigenvector in this analysis, capturing the broadest spatial pattern. In our case, MEM1 showed a west-east separation, into two main clusters. The first group included CHA, PTZ, and most of CTZ basins, while the second group included BAL and MEX, and the most eastern populations of CTZ (Fig. 3A). The MEM2 (r = 0.0451, P = 0.017) represents the second eigenvector, capturing a fine-scale spatial structure. Our results, MEM2 identified the most geographically distant basins as the most differentiated (Fig. 3B). Contemporary migration rate analysis showed that the CHA contributed most strongly to gene flow to adjacent basins. CHA provides 15% of migrants to CTZ, and 11% of migrants to PTZ. The MEX basin is the second largest contributor to the CTZ, with 14% of migrants, and to PTZ with 9% of migrants, while other basins had lower migration rates (Fig. 4; Appendix S3). The Mantel test was not significant (r = 0.07; P *> 0.05*), indicating no relationship between genetic and geographic distances.

Habitat suitability model

The ENM result showed that the final uncorrelated variables were minimum temperature of the coldest month (BIO6: 41.9%), precipitation seasonality (BIO15:19.2%), temperature annual range (BIO7: 12.5%), precipitation of the wettest quarter (BIO16: 11.7%), precipitation of the warmest quarter (BIO18: 8.4%), mean temperature of the driest quarter (BIO9: 4.2%), and precipitation of the coldest quarter (BIO19: 6.3%). The species distribution model identified the center-south region of the country (including eastern Michoacán, Mexico City, and northern Morelos) as having the most extensive suitable habitat, covering an area of 79,103 km² (Appendix S4). The selected TPR+TRN model (P = 0.144751), which included product and threshold features, highlighting interactions among climatic variables and suggested abrupt ecological limits in the species' distribution. The model showed excellent predictive performance (AUC = 0.9465111). The metric used to evaluate the efficiency of machine learning in the species distribution model was TSS = 0.6119, indicating that the model is good for predicting presences and absences. The obtained value of EI = 36 indicated optimal habitat suitability for *B. cuneata* (Coetzee et al. 2009).

Landscape genetics

Gravity model analyses across spatial scales (1,000-5,000 m) revealed scale-dependent predictors of functional connectivity for the between-site factors, while the at-site factors (slope steepness and east aspect) had no effect on any spatial scale. The best model selected for 1,000 and 2,000 m was Rough, which showed the lowest AICs and highest PVE values (46.7% and 45.1%, respectively) (Table 3). For the 3,000 and 4,000 m scales, the Comb3 model (TDF, TF, Niche, and Rough) was selected as the best-performing model with the highest PVE values (52.4% and 49.5 %, respectively) and the lowest AICs. Particularly, at 3000 m, Rough had the highest significant and positive relative importance (Cohen´s D = 0.44), followed by TDF (Cohen´s D = 0.38). In contrast, at 4,000m, TDF showed greater relative importance (Cohen´s D = 0.40) than Rough (Cohen´s D = 0.37). Lastly, at 5,000 m, Comb2 (TDF and TF) was selected as the best-performing model with the lowest AIC, although it did not show the highest PVE (12.4%). TDF showed positive and greater relative importance (Cohen´s D = 0.54) than TF (Cohen´s D = - 0.33), which had a negative effect (Table 3, Appendix S5).

Discussion

Our landscape genetics study of *B. cuneata* across central Mexico showed weak to moderate spatial patterns of genetic structure among the five hydrological basins, and with asymmetrical contemporary migration rates. Our gravity model analysis of functional connectivity identified terrain roughness and tropical dry forest (TDF) cover as scale-dependent predictors of gene flow in *B. cuneata,* with largest importance of TDF at a regional scale. The following sections provide a detailed discussion of the main findings.

Genetic diversity and patterns of spatial genetic structure

Our results revealed high genetic diversity across all five basins, with nucleotide diversity (π) values exceeding those reported for other tree species, such as *Pinus pinaster*, *P. radiata* (π = 0.00186), *P. taeda* (π = 0.00853), *Pseudotsuga menziesii* (π = 0.00655), and *Eucalyptus pellita*) (π = 0.00066, Wang *et al*., 2023). Among the basins, CTZ exhibited the highest genetic diversity, whereas MEX showed the lowest. This pattern agrees with field observations: in Michoacán, *B. cuneata* populations, particularly in the CTZ basin, maintain high densities, and the *Bursera* genus is common in remnant tropical dry forest fragments (Rzedowski and Medina-Lemos, 2023). In contrast, abundance has declined markedly in MEX because of rapid urbanization pressures (Carreón and Soler, 2007). Notably, we found substantially higher inbreeding coefficients (F_{IS}) in *B. cuneata* compared to relatives such as *B. simaruba* (F_{IS} = 0.024; Dunphy and Hamrick, 2007). The highest values occurred in peripheral basins, particularly BAL (F_{IS} = 0.44) and CHA (F_{IS} = 0.45). Specifically, populations of the CHA basin, such as La Alberca Protected Natural Area, persist within intensified agricultural landscapes with extensive livestock grazing (Ramírez-Ramos, 2023), which exacerbates genetic isolation.

Genetic structure analyses, including Bayesian and Multivariate clustering approaches along with Moran's Eigenvector Maps, revealed two hierarchical patterns of differentiation: (1) five genetic clusters with higher differentiation of BAL, and (2) a broader west-east genetic differentiation across the species' range. Geographically proximate basins (CHA, PTZ, and CTZ) showed higher admixture, while BAL and MEX showed higher genetic differentiation. BAL is a recognized center of endemism for the *Bursera* genus (Espinosa et al., 2006), and its high differentiation may be attributed to its large size, high topographic and environmental complexity, and steep climatic gradients ranging from warm, dry conditions in eastern Michoacán to cooler, stable environments in Morelos (Toledo-Manzur, 1984; Espinosa et al., 2006; Gámez et al., 2014; Steinmann, 2021). Contemporary migration rates support this pattern, and although asymmetrical gene flow occurs among distant basins (e.g., MEX, CHA, and PTZ), connectivity with BAL is reduced.

At a regional scale, Moran's Eigenvector Maps highlighted significant west-east genetic differentiation. Although the species is spatially aggregated within TDF fragments, where gene flow is more likely among nearby populations than distant ones, we did not detect isolation by distance (IBD). This suggests that geographic distance alone does not explain patterns of genetic structure. Instead, the west-east divergence may reflect a shared biogeographic history. A large portion of the distribution of *B. cuneata* is found within the Trans-Mexican Volcanic Belt (TVB), a transition zone between the Neotropical and Nearctic regions (Gámez et al., 2012). Similar genetic patterns in TVB taxa have been reported in Asteraceae (e.g., *Acourtia lepidopoda*, *Stevia hintonii*, and *Microspermum flaccidum*; Villaseñor et al. 2021), oaks (*Quercus deserticola*, Rodríguez-Gómez et al. 2018), and rodents (*Peromyscus maniculatus*, Léon-Tapia et al. 2021), which are likely the result of the TVB's gradual geological development, where volcanic activity began in the west during the Miocene, while eastern regions emerged later in the Pliocene-Pleistocene (Mastretta-Yanes et al. 2015). Together, these results reflect that the *B. cuneata* spatial genetic patterns reflect both contemporary and historical processes. Future studies should include phylogeographical approaches to evaluate the role of biogeographic barriers, particularly TVB's Miocene-Pliocene fragmentation, and genotype-environment associations (GEA) of candidate selective loci underlying local adaptation to unique microsite conditions across the species distribution.

Drivers of functional connectivity

Gravity model results demonstrate that *B. cuneata* gene flow responds differentially to landscape features across spatial scales. At smaller scales, 1,000 to 3,000 m, terrain roughness emerged as the most significant factor driving functional connectivity, while at broader scales (4,000 to 5,000 m), thepresence of the native habitat (TDF) became more important. The positive association with rugged topography aligns with *B. cuneata* preference for topographically complex volcanic landscapes (locally called "malpaíses") (Rzedowski and Guevara-Féfer 1992). These habitats harbor specialized flora with traits adapted to rocky, nutrient-poor soils and tolerance to drought (Trejo and Dirzo, 2002; Méndez-Toribio et al. 2017). Notably, the proportion of TDF cover at larger scales (> 4,000 m) was the main driver of functional connectivity for *B. cuneata*, consistent with the strong ecological specialization of *Bursera* on this ecosystem (Rzedowski and Guevara-Féfer 1992; De Nova et al., 2011). This was further supported by the ecological niche model (ENM), which showed strong spatial congruence between areas of high habitat suitability for *B. cuneata* and the distribution of TDF in the region. The ENM result underscores TDF's role as a critical factor for maintaining functional connectivity at regional scales, where terrain roughness declines in importance beyond 3,000 m, likely reflecting species-specific dispersal dynamics. Although seed dispersal and pollination studies in *B. cuneata* are lacking, studies for other *Bursera* species suggest that birds are the primary seed vector, and with secondary dispersal by small reptiles and mammals (Almazán-Núñez et al. 2021), while pollination is carried out by flies, bees, and beetles (Rivas-Arancibia et al. 2015). These dispersal mechanisms may explain why terrain roughness does not restrict the movement of gene flow by vectors, as they can navigate rugged topography, highlighting the availability of TDF habitat at larger scales as the key factor enabling gene flow across fragmented landscapes.

At broader scales (>4,000 m), the temperate forest acted as a dispersal barrier for *B. cuneata*, even though the species occasionally occurs in transitional zones between temperate forest and tropical dry forest. This barrier effect is likely due to the cooler, humid, and frost-prone conditions in temperate forests, which are unsuitable for the establishment of *Bursera* species (Alfaro Reyna et al., 2019). These climatic constraints reinforce TDF as the primary habitat of *B. cuneata*. In contrast, other landscape factors, such as agricultural and urban land covers, had no significant effects on functional connectivity, despite their increasing presence in the region. This absence of signal may reflect time-lagged genetic responses to recent anthropogenic changes, as long-lived plant species often exhibit delayed genetic effects following habitat fragmentation (Aguilar et al., 2008; Aavik *et al*., 2019).

Conservation implications

Land-use changes are the main threats to the persistence of TDF in Mexico (Koleff et al. 2009), risking long-term genetic erosion through reduced gene flow, increased inbreeding, and genetic drift of TDF forest tree species. Our results suggest that conserving TDF remnant forests is critical for maintaining functional connectivity in *Bursera cuneata*, particularly among the CHA-PTZ-CTZ basins in Michoacán, which are important genetic reservoirs. Even in urbanized regions like Mexico City, remnant trees in protected natural parks (La Reserva del Pedregal de San Ángel) may function as stepping-stones for pollinator and seed vector movements, providing key connectivity between urban and rural populations. Other important areas to focus on are the habitat connection between MEX and BAL basins through the Chichinautzin Biological Corridor, which is an important zone harboring biodiversity (Flores-Estrella et

al. 2007), including endemic species like *Bursera cuneata*. We propose protecting and prioritizing crucial TDF remnants in Michoacan and the Chichinautzin Corridor to maintain large-scale gene flow by integrating urban natural parks as important links to prevent genetic isolation between urban and rural *B. cuneata* populations.

Conclusions

This study provided a comprehensive landscape genomic assessment of *B. cuneata*, which combined extensive population sampling across the species' range, using SNP markers. Our main findings showed high levels of genetic diversity with patterns of genetic structure among basins and a historical west-east genetic divergence. Our analysis underscores that functional connectivity is a scale-dependent process. Specifically, terrain roughness was the primary factor of connectivity at finer scales (1,000–3,000 m), while tropical dry forest cover became the main driver at broader scales (>4,000 m). These findings highlight the need for targeted conservation measures that preserve functional connectivity for *B. cuneata* by promoting TDF connectivity across regional scales, especially in landscapes undergoing rapid fragmentation.

Declarations

Funding

This study was funded by the Secretaria de Ciencias, Humanidades, Tecnología e Innovación (SECIHTI) (CB2016-283237).

Acknowledgements

We thank for their assistance in collecting leaf material to Benjamín Castillo Ponce, Eduardo Quintero Melecio, Bruno A. Gutiérrez Becerril, Victor Reyes Pino, Stephanie Aguilera López, Tania Andrade Ortiz, Sergio Nicasio Arzeta, Sergio Zamudio, and several field assistants from local communities. Also, thanks to Mayra Castro Morales for her assistance in DNA extractions, and Ingrid Lara and Antonio González Rodríguez for the DNA quantification using Qubit.

Contributions

YR and MSZ conceptualized the study. YR conducted field work and provided funding for the project; MSZ, BO, and YR conducted data analysis; MSZ wrote the manuscript; all authors contributed to editing.

Competing Interest

The authors have no relevant financial or non-financial interests to disclose.

Data Availability

The SNP data for 227 individuals at 10,499 loci will be deposited on Dryad upon acceptance.

References

1. Aavik T, Thetloff M, Träger S, Hernández-Agramonte IM, Reinula I, Pärtel M (2019) Delayed and immediate effects of habitat loss of the genetic diversity of the grassland plant *Trifolium montanum*. Biodivers Conserv 28(12): 3299-3319. DOI: 10.1007/s10531-019-01822-8
2. Aguilar R, Quesada M, Ashworth L, Herrerias-Diego Y, Lobo J (2008) Genetic consequences of habitat fragmentation in plant populations: susceptible signals in plant traits and methodological approaches. Mol Ecol 17(24): 5177-5188. DOI: 10.1111/j.1365-294X.2008.03971.x
3. Akaike H (1973) Maximum likelihood identification of Gaussian autoregressive moving average models. Biometrika 60(2): 255-265. DOI: 10.1093/biomet/60.2.255
4. Alfaro Reyna T, Martínez-Vilalta J, Rentana . (2019) Regeneration patterns in Mexican pine-oak forests. For Ecosyst 6(1): 50. DOI: 10.1186/s40663-019-0209-8
5. Allouche O, Tsoar A, Kadmon R (2006) Assessing the accuracy of species distribution models: Prevalence, kappa and the true skill statistic (TSS). J Appl Ecol 43(6): 1223-1232. DOI: 10.1111/j.1365-2664.2006.01214.x
6. Almazán-Núñez RC, Eguiarte LE, Arizmendi MC, Corcuera P (2016) *Myarchus* flycatchers are the primary seed dispersers of *Bursera longipes* in a Mexican dry forest Peer J 4: e2126. DOI: 10.7717/peerj.2126
7. Almazán-Núñez RC, Rodríguez-Godínez R, Méndez-Bahena A, Pineda-López R (2021) Las aves frugívoras y su papel en la restauración pasiva del bosque tropical caducifolio del sur de México: Un caso de estudio con la cactácea *Pachycereus weberi*. In: Mercado-Silva N, Del Val EK, eds. Manejo y Conservación de Fauna Nativa en Ambientes Antropizados. Mexico: Universidad Autónoma de Querétaro, pp 61-83.
8. Auffret AG, Rico Y, Bullock JM, Hooftman DAP, Pakeman RJ, Soons MB et al. (2017) Plant functional connectivity - integrating landscape structure and effective dispersal. J Ecol105(2): 1648-1656. DOI: 10.1111/1365-2745.12742
9. Balzotti CS, Asner GP, Adkins ED, Parsons EW (2020) Spatial drivers of composition and connectivity across endangered tropical dry forests. J Appl Ecol 57(8): 1593-1604. DOI: 10.1111/1365-2664.13632
10. Becerra JX (2003) Evolution of Mexican *Bursera* (Burseraceae) inferred from ITS, ETS, and 5S nuclear ribosomal DNA sequences. Mol Phylogenet Evol 26(2): 300-309. DOI: 10.1016/S1055-7903(02)00256-7
11. Becerra JX (2005) Timing the origin and expansion of the Mexican tropical dry forest. PNAS 102(31): 10919-10923. DOI: 10.1073/pnas.0409127102

12. Becerra JX, Venable DL (1999) Nuclear Ribosomal DNA Phylogeny and ITS implications for evolutionary trends in Mexican *Bursera* (Burseraceae). Ame J Bot 86(7): 1047-1057. DOI: 10.2307/2656622
13. Becerra JX. Venable DL (2008) Sources and Sinks of Diversification and Conservation Priorities of the Mexican Tropical Dry Forest. Plos one 3: e3436. DOI: 10.1371/journal.pone.0003436
14. Bezaury-Creel E (2010) Selvas Secas del Pacífico mexicano. In: Ceballos G, Martínez L, García A, Espinoza E, Bezaury-Creel E, Dirzo R, eds. Diversidad, amenazas y áreas prioritarias para la conservación de las Selvas Secas del Pacífico de México. Mexico: Fondo de Cultura Económica, pp 21-24.
15. Blackie R, Baldauf C, Gautier D, Gumbo D, Kassa H, Parthasarathy N, et al. (2014) In: Tropical dry forests: the state of global knowledge and recommendations for future research. Discussion paper. Bogor, Indonesia. CIFOR, pp 40.
16. Caballero M, Lozano García S, Vázquez Selem L, Ortega B (2010) Evidencias de cambio climático y ambiental en registros glaciales y en cuencas lacustres del centro de México durante el último máximo glacial. Bol Soc Geol Mex 62(3): 359-377. DOI:10.18268/BSGM2010v62n3a4
17. Céspedes L, Ortiz E, Villaseñor JL (2018) La familia Asteraceae en la Reserva Ecológica del Pedregal de San Ángel, Ciudad de México, México. Rev Mex Biodiv 89(1): 193-207. DOI: 10.22201/ib.20078706e.2018.1.2203
18. Cobos ME, Townsend Peterson A, Barve N, Osorio-Olvera L (2019) Kuenm: an R package for detailed development of ecological niche models using Maxent. PeerJ 7: e6281. DOI: 10.7717/peerj.6281
19. Coetzee BW, Robertson MP, Erasmus BF, Van Rensburg BJ, Thuiller W (2009) Ensemble models predict important Bird Areas in Southern Africa will become less effective for conserving endemic birds under climate change. Glob Ecol Biogreogr 18(6): 701-710. DOI: 10.1111/j.1466-8238.2009.00485.x.
20. Cruzan MB, Hendrickson EC (2020) Landscape Genetics of Plants: Challenge and Opportunities. Plant Commun 1: 100100. DOI: 10.1016/j.xplc.2020.100100
21. Cué-Bär E, Villaseñor JL, Arredondo-Amezcua L, Cornejo-Tenorio G, Ibarra-Manríquez G (2006) La flora arbórea de Michoacán, México. Bol Soc Bot México 78(78): 47-81.
22. Cultid-Medina CA, Rico Y (2020) Los aliados emplumados de los Copales y Cuajiotes de México: Aves y la dispersión de semillas de Bursera. Rev Digit Univ 21(2): DOI: 10.22201/codeic.16076079e.2020.v21n2.a5
23. De León-Mojarro B, Medina-Mendoza R, González-Casillas A (2001) Natural Resources Management in the Lerma-Chapala Basin. In: Hansen AM, Van Afferden M, *eds*. The Lerma-Chapala Watershed US: Springer, pp 59-92. DOI: 10.1007/978-1-4615-0545-7_3
24. Dormann CF, Elith J, Bacher S, Buchmann C, Carl G, Carré G et al. (2012) Collinearity a review of methods to deal with it and a simulation study evaluating their performance. Echography 36(1): 027-046. DOI: 10.1111/j.1600-0587.2012.07348.x
25. De-Nova JA, Medina R, Montero JC, Weeks A, Rosell JA, Olson ME, et al. (2012). Insights into the historical construction of species-rich Mesoamerican seasonally dry tropical forests: the diversification of Bursera (Burseraceae, Sapindales). New Phytologist, 193(2): 276-287. DOI: https://doi.org/10.1111/j.1469-8137.2011.03909.x
26. Drake E, Farid A, Hanna Y, Ku J (2020) Acorn woodpeckers (*Melanerpes formicivorus*) exhibit more predator avoidance behavior post-fire. CEC Research DOI: 10.21973/N3H669
27. Dunphy BK, Hamrick JL (2007) Estimation of gene flow into fragmented populations of *Bursera simaruba* (Burseraceae) in the dry-forest life zone of Puerto Rico. Am J Bot 94(11): 1786-1794. DOI: 10.3732/ajb.94.11.1786
28. Dyer J (2009) Assessing topographic patterns in moisture use and stress using water balance approach. Landsc Ecol 24(3): 391-403. DOI: 10.1007/s10980-008-9316-6
29. Eisenlohr PV, Alves LF, Bernacci LC, Padgurschi MCG, Torres RB, Prata FAM et al. (2013) Disturbance, elevation, topography and spatial proximity drive vegetation patterns along an altitudinal gradient of a top biodiversity hotspot. Biodiv Conserv 22(12): 2767-2783. DOI: 10.1007/s10531-013-0553-x
30. Espinosa D, Llorente J, Morrone JJ (2006) Historical biogeographical patterns of the species. of *Bursera* (Burseraceae) and their taxonomic implications. J Biogeogr 33(11): 1945-1958. DOI: 10.1111/j.1365-2699.2006.01566.x
31. Evans JS, Murphy MA (2022) *GeNetIt*: R package version 0.1-5.
32. Flores-Estrella H, Yussim S, Lomnitz C (2007) Seismic response of the Mexico City Basin: A review of twenty years of research. Nat Hazards 40: 357-372. DOI: 10.1007/s11069-006-0034-6
33. François O, Martins H, Caye K, Schoville SD (2016) Controlling false discoveries in genome scans for selection. Mol Ecol 25(2): 454-469. DOI: 10.1111/mec.13513
34. Frichot E, François O (2015) LEA: An R package for landscape and ecological association studies. Methods Ecol Evol 6(8): 925-929. DOI: 10.1111/2041-210X.12382
35. Fuentes ACD, Samain SM, Martínez-Salas E (2019) Copal *Bursera cuneata* has most recently been assessed for The IUCN Red List of Threatened Species in 2019: e.T137371772A137376559. http://dx.doi.org/10.2305/IUCN.UK.2019- 3.RLTS.T137371772A137376559.en visit on 18 April 2025.
36. Galpern P, Peres-Neto PR, Polfus J, Manseau M (2014) MEMGENE: Spatial pattern detection in genetic distance data. Methods Ecol Evol 5(10): 1116-1120. DOI: 10.1111/2041-210X.12240
37. Gámez N, Escalante T, Rodríguez G, Linaje M, Morrone JJ (2012) Biogeographic characterization of the Transmexican Volcanic Belt and analysis of the distributional patterns of the mammal fauna. Rev Mex Biodiv 83(1): 258-272. DOI: 10.22201/ib.20078706e.2012.1.786
38. Gámez N, Escalante T, Espinosa D, Eguiarte LE, Morrone JJ (2014) Temporal dynamics of areas of endemism under climate change: a case study of Mexican *Bursera* (Burseraceae). J Biogeogr 41(5): 871-881. DOI: 10.1111/jbi.12249
39. Goudet J (2005) HIERFSTAT, a package for R to compute and test hierarchical *F*-statistics. Mol Ecol Notes 5(1): 184-186. DOI: 10.1111/j.1471-8286.2004.00828.x

40. Grizzard M, Shaw AZ (2017) Effect Size. In: Matthes J, Davis CS, Potter RF, eds. The International Encyclopedia of Communication Research Methods US: John Wiley & Sons Inc. pp 1-8. Wiley. DOI: 10.1002/9781118901731.iecrm0076
41. Gruber B, Unmack PJ, Berry O, Georges A (2018) dartR: an R package to facilitate analysis of SNP data generated from reduced representation genome sequencing. Mol Ecol Resour 18(3): 691-699. DOI: 10.1111/1755-0998.12745
42. Healey A, Furtado A, Cooper T, Henry RJ (2014) Protocol: a simple method for extracting next-generation sequencing quality genome DNA from recalcitrant plant species. Plant Methods 10(1): 21. DOI: 10.1186/1746-4811-10-21
43. Hernández-Oria JG (2007) Desaparición del Bosque Seco en El Bajío mexicano: Implicaciones del ensamblaje de especies y grupos funcionales en la dinámica de una vegetación amenazada. Zonas Áridas 11(1):13-31**.** DOI:10.21704/za.v11i1.201
44. Hernández-Pérez E, González-Espinosa M, Trejo I, Bonfil C (2011) Distribución del género *Bursera* en el estado de Morelos, México y su relación con el clima. Rev Mex Biodiv 82(3):964-976. DOI: 10.22201/ib.20078706e.2011.3.694
45. Hijmans, R (2022) raster: Geographic Data Analysis and Modeling. R package version 3.5. https://github.com/rspatial/raster visit on 4 May 2025.
46. Holderegger R, Buehler D, Gugerli F, Manel S (2010) Landscape genetics of plants. Trends Plant Sci 15(12):675-683. DOI: 10.1016/j.tplants.2010.09.002
47. INEGI, Insttituto Nacional de Estadística y Geografía (2021) Geografía y Medio Ambiente. Hidrología. https://www.inegi.org.mx/temas/hidrologia/#descargas visit on 17 Feb 2024.
48. Israde-Alcántara I, Garduño-Monroy VH, Fisher CT, Pollard HP, Rodríguez-Pascua MA (2005) Lake level change, climate, and the impact of natural events: The role of seismic and volcanic events in the formation of the Lake Patzcuaro Basin, Michoacan, Mexico. Quat Int 135(1):35-46. DOI: 10.1016/j.quaint.2004.10.022
49. Jombart T, Ahmed I (2011) *adegenet 1.3-1*: new tools for the analysis of genome-wide SNP data. Bioinformatics 27(21):3070-3071. DOI: 10.1093/bioinformatics/btr521
50. Kamvar ZN, Tabima JF, Grünwald NJ (2014) *Poppr*: an R package for genetic analysis of populations with clonal, partially clonal, and/or sexual reproduction. PeerJ 2: e281. DOI: 10.7717/peerj.281
51. Knaus BJ, Grünwald NJ (2017) *VCF*: a package to manipulate and visualize variant call format data in R. Mol Ecol Resour 17(1):44-53. DOI: 10.1111/1755-0998.12549
52. Koleff P, Tambutti M, March IJ, Esquivel C, Cantú C, Lira-Noriega A et al. (2009) Identificación de prioridades y análisis de vacíos y omisiones en la conservación de la biodiversidad de México. In: Capital natural de México, vol. II: Estado de conservación y tendencias de cambio. Mexico: CONABIO, pp 651-718.
53. Kriticos DJ, Maywald GF, Yonow T, Zurcher EJ, Herrmann Ni, Sutherst RW (2015) *CLIMEX Version 4:* Exploring the Effects of Climate on plants, animals and diseases. Canberra: CSIRO, pp 184.
54. Kuster RD, Yencho GC, Olukolu BA (2021) ngsComposer: An automated pipeline for empirically based NGS data quality filtering. Brief Bioinform 22(5): bbab092. DOI: 10.1093/bib/bbab092
55. Léon-Tapia M, Fenández JA, Rico Y, Cervantes FA, Espinosa de los Monteros A (2020) A new mouse of the *Peromyscus maniculatus* species complex (Cricetidae) from the highlands of central Mexico. J Mammal 101(4):1117-1132. DOI: 10.1093/jmammal/gyaa027
56. Luft-Dávalos R, Álvarez Icaza P (2009) Artesanías y medio ambiente. Mexico: Fondo Nacional para el Fomento de las Artesanías (FONART).
57. Mastretta-Yanes A, Moreno-Letelier A, Piñero D, Jorgensen TH, Emerson BC (2015) Biodiversity in the Mexican highlands and the interaction of geology, geography and climate within the Trans-Mexican Volcanic Belt. J Biogeogr 42(9):1586-1600. DOI: 10.1111/jbi.12546
58. Maya-Elizarrarás M, Rico Y, Cultid-Medina CA (2024) Copales, cuajiotes y sus visitantes. Ecofronteras 28(20):20-24.
59. Méndez-Toribio M, Martínez-Cruz J, Cortés-Flores J, Rendón-Sandoval FJ, Ibarra-Manríquez G (2014) Composition, structure and diversity of Tziritzícuaro tropical dry forest tree community, Balsas Watershed, Michoacán, México. Rev Mex Biodiv85(4):1117-1128. DOI: 10.7550/rmb.43457
60. Méndez-Toribio M, Meave JA, Zermeño-Hernández I, Ibarra-Manríquez G (2016) Effects of slope aspect and topographic position on environmental variables, disturbance regime and tree community attributes in a seasonal tropical dry forest. J Veg Sci 27(6):1094-1103. DOI: 10.1111/jvs.12455
61. Méndez-Toribio M, Ibarra-Manríquez G, Navarrete-Segueda A, Paz H (2017) Topographic position, but not slope aspect, drives the dominance of functional strategies of tropical dry forest tress. Environ Res Lett 12(8)**:** 085002. DOI: 10.1088/1748-9326/aa717b
62. Mendoza-Ponce A, Corona-Núñez RO, Galicia L, Kraxner F (2019) Identifying hotspots of land use cover change under socioeconomic and climate change scenarios in Mexico. Ambio 48(4):336-349. DOI: 10.1007/s13280-018-1085-0
63. a.Mesa-Sierra N, Laborde J, Chaplin-Kramer R, Escobar F (2022) Carbon stocks in a highly fragmented landscape with seasonal dry tropical forest in the Neotropics. For Ecosyst 9:100016. DOI: 10.1016/j.fecs.2022.100016
64. b. Mesa-Sierra N, De la Peña-Domene M, Campo J, Giardina CP (2022) Restoring Mexican Tropical Dry Forests: A National Review. Sustainability 14(7):3937. DOI: 10.3390/su14073937
65. Metcalfe SE, Davies SJ, Braisby JD, *et al*. O'Hara SL (2007) Long and short-term change in the Patzcuaro Basin, central Mexico. PALAEO 247(3):272-295. DOI: 10.1016/j.palaeo.2006.10.018
66. Miller KE (2014) Great crested flycatcher (*Myiarchus crinitus*) nest-site selection and nesting success in tree cavities. Fla Field Nat 42(2):45-90.
67. Montúfar-López A (2016) Copal of *Bursera bipinnata.* A Ritual Mesoamerican Resin. Trace 70:45-77. DOI: 10.22134/trace.70.2016.39
68. Murphy MA, Evans JS, Storfer A (2010) Quantifying *Bufo boreas* connectivity in Yellowstone National Park with landscape genetics. Ecol 91(1):252-261. DOI: 10.1890/08-0879.1
69. Murphy PG, Lugo AE (1986) Ecology of tropical dry forest. Annu Rev Ecol Syst 17(1):67-88. DOI: 10.1146/annurev.es.17.110186.000435

70. Nei M (1978) Estimation of Average Heterozygosity and Genetic Distance from a Small Number of Individuals. Genetics 89(3):583-590. DOI: 10.1093/genetics/89.3.583
71. Oksanen J, Blanchet FG, Friendly M, Kindt R, Legendre P, McGlinn D et al. (2020) *Vegan 2.5-7*: Community Ecology Package.
72. Osorio-Olvera L, Lira-Noriega A, Soberón J, Townsend-Peterson A, Falconi M, Contreras-Díaz RG et al. (2020) NTBOX: An R package with graphical user interface for modelling and evaluating multidimensional ecological niches. Methods Ecol Evol 11:1199-1206. DOI: 10.1111/2041-210X.13452
73. Pagaza-Calderón EM & Fernández-Nava R (2004) La familia Bombaceae en la cuenca del Río Balsas, México. Polibot 17:71-102.
74. Phillips SJ, Anderson RP, Dudík M, Schapire RE, Blair ME (2017) Opening the black box: an open-source release of Maxent. Ecography 40(7):887-893. DOI: 10.1111/ecog.03049
75. Powers JS, Feng X, Sanchez-Azofeifa A, Medvigy D (2018) Focus on tropical dry forest ecosystems and ecosystem services in the face of global change. Environ Res Lett 13(9):090201. DOI: 10.1088/1748-9326/aadeec
76. Privé F, Luu K, Vilhjálmsson BJ, Blum MGB (2020) Performing Highly Efficient Genome Scans for Local Adaptation with R Package pcadapt Version 4. Mol Biol Evol 37(7):2153-2154. DOI: 10.1093/molbev/msaa053
77. Quisehuatl-Medina A, Webb CO, Hubbel SP, Méndez-Toribio M, González-Zaragoza C López-Toledo L (2023) Topography drives tree–habitat association and functional and phylogenetic structure in the Northernmost tropical dry forest of the Americas. Plant Ecol Divers 16(3):203-220 DOI: https://doi.org/10.21203/rs.3.rs-404564/v1
78. Ramírez-Ramos F (2023) Flora y vegetación del Área Natural Protegida La Alberca, municipio Tacámbaro, Michoacán, México. Act Bot Mex 130:e2209. DOI: 10.21829/abm130.20232209
79. Rendón-Sandoval FJ, Casas A, Sinco-Ramos PG, Garcia-Frapolli E, Moreno-Calles AI (2021) Peasants' Motivations to Maintain Vegetation of Tropical Dry Forests in Traditional Agroforestry Systems from Cuicatlán, Oaxaca, Mexico. Front Environ Sci 9:682207. DOI: 10.3389/fenvs.2021.682207
80. Rico Y, Lorenzana GP, Benítez-Pineda CA, Olukolu BA (2022) Development of Genomic Resources in Mexican *Bursera* (Section: *Bullockia*: Burseraceae): Genome Assembly, Annotation, and Marker Discovery for Three Copal Species. Genes 13(10):1741 DOI: 10.3390/genes13101741
81. Rivas-Arancibia SP, Bello-Cervantes E, Carrillo-Ruiz H, Andrés-Hernández AR, Figueroa-Castro, Guzmán-Jiménez S (2015) Variaciones en la comunidad de visitadores florales de *Bursera copallifera* (Burseraceae) a lo largo de un gradiente de perturbación antropogénica. Rev Mex Biodiv 86(1):178-187.
82. Rodríguez-Gómez F, Oyama K, Ochoa-Orozco M, Mendoza-Cuenca L, Gaytán-Legaria R, González-Rodríguez A (2018) Phylogeography and climate-associated morphological variation in the endemic white oak *Quercus deserticola* (Fagaceae) along the Trans-Mexican Volcanic Belt. Botany 96(2):121-133. DOI: 10.1139/cjb-2017-0116
83. Romero-Báez Ó, Murphy MA, Díaz de la Vega-Pérez AH, Vázquez-Domínguez E (2024) Environmental and anthropogenic factors mediating the functional connectivity of the mesquite lizard along the eastern Trans-Mexican Volcanic Belt. Mol Ecol 33(16):e17469. DOI: 10.1111/mec.17469
84. Rosell JA, Olson ME, Weeks A, De-Nova JA, Medina-Lemos R, Pérez-Camacho J et al. (2010) Diversification in species complexes: Tests of speces orgin and delimitation in the *Bursera simaruba* clade of tropical trees (Burseraceae). Mol Phylogenet Evol 57(2):798-811. DOI: 10.1016/j.ympev.2010.08.004
85. Rzedowski J (1991) Diversidad y origen de la flora fanerogámica de México. Act Bot Mex 14:3-21.
86. Rzedowski J (2006) Capítulo 12. Bosque tropical caducifolio. In: Rzedowski J, *ed*. Vegetación de México. Mexico (CONABIO, pp 200-214.
87. Rzedowski J, Guevara-Féfer F (1992) Burseraceae. Flora del Bajío y de regiones adyacentes 3:1-46.
88. Rzedowski J. Kruse H (1979) Algunas tendencias evolutivas en *Bursera* (Burseraceae). Taxon 28(1):103-119.
89. Rzedowski J. Medina-Lemos R (2023) *Bursera*. In: Rzedowski J. Medina-Lemos R, *eds*. Las especies de Bursera Jacq. ex L. en el Occidente de México. Mexico: UNAM IB, pp169.
90. Steinmann VW (2021) Flora and vegetation of the Zicuirán-Infiernillo Biosphere Reserve, Michoacan, Mexico. Bot Sci 99(3):661-707. DOI: 10.17129/botsci.2706
91. Toledo-Manzur CA (1984) Contribuciones a la flora de Guerrero: tres especies nuevas del género *Bursera* (Burseraceae). Biotica 9(4): 441-449.
92. Trejo I, Dirzo R (2000) Deforestation of seasonally dry tropical forest: A national and local analysis in Mexico. Biol Conserv 94(2):133-142. DOI: 10.1016/S0006-3207(99)00188-3
93. Trejo I, Dirzo R (2002) Floristic Diversity of Mexican seasonally dry tropical forest. Biodiv Conserv 11:2063-2084. DOI: 10.1023/A:1020876316013
94. Villaseñor JL, Ortíz E, Juárez (2021) Transition zones and biogeographic characterization of endemism in three biogeographic provinces of Central Mexico. Bot Sci 99(4): 938-954. DOI: 10.17129/botsci.2768
95. Wang C, Lan J, Wang J, He W, Lu W, Lin Y et al. (2023) Population structure and genetic diversity in *Eucalyptus pellita* based on SNP markers. Front Plant Sci 14:1278427. DOI: 10.3389/fpls.2023.1278427
96. Weeks A, Simpson BB (2007) Molecular phylogenetic analysis of *Commiphora* (Burseraceae) yields insight on the evolution and historical biogeography of an "impossible" genus. Mol Phylogenet Evol 42(1):62-79. DOI: 10.1016/j.ympev.2006.06.015
97. Wilson GA, Rannala B (2003) Bayesian Inference of recent migration rates using multilocus geno-types. Genetics 163(3):1177-1191.
98. Yencho GC, Olukolu BA (2022) Compositions and Methods Related to Quantitative Reduced Representation Sequencing. Available online: https://patents.google.com/patent/US20220243267A1/ visit on 20 May 2025.
99. Yoon S, Lee WH (2023) Application of true skill statistics as a practical method for quantitatively assessing CLIMEX performance. Ecol Indic 146:109830. DOI: 10.1016/j.ecolind.2022.109830

Tables

Table 1. Genetic diversity estimates for the five hydrological basins: Lerma-Chapala basin (CHA), Patzcuaro Lake (PTZ), Cuitzeo Lake (CTZ), Balsas River basin (BAL) and Mexico´s basin (MEX). We calculated genetic diversity using the 10,499 SNPs. The total number of individuals (*N*), we calculated the private alleles per basin (*Ap*), the number total alleles (*A*), the nucleotide diversity (π). We calculated the observed heterozygosity (Ho), unbiased expected heterozygosity (*uHe*), and the inbreeding coefficient for each basin (F_{IS}).

Locality	ID	N	Ap	A	π	Ho	uHe	F_{IS}
Lerma-Chapala	CHA	14	6	16230	0.1787	0.0988	0.1682	0.4487
Patzcuaro	PTZ	87	314	20404	0.1919	0.1267	0.1906	0.3396
Cuitzeo	CTZ	88	555	20650	0.3117	0.1337	0.1932	0.3863
Balsas River	BAL	28	597	18620	0.1964	0.1133	0.1916	0.4436
Mexico	MEX	10	2	14876	0.158	0.0894	0.1441	0.4232

Table 2. AMOVA results in the 33 populations of *B. cuneata* and between five hydrological basins: Lerma-Chapala basin (CHA), Patzcuaro Lake (PTZ), Cuitzeo Lake (CTZ), Balsas River basin (BAL) and Mexico´s basin (MEX). Analyzed groups: 1) No predefined groups. 2) populations grouped in the five basins. * $P < 0.01$ ** $P < 0.001$

	df	Estimated variance	%	Statistics
Among populations	1	0.11	1.1	$F_{ST} = 0.09$
Within populations	225	0.15	98.9	$F_{ST} = 0.01$
Total	226	0.26	100	
Between basins	4	1.51	8.51	$F_{CT} = 0.009$*
Between localities within basins	32	2.85	39.46	$F_{ST} = 0.008$*
Within populations	190	2.99	52.03	$F_{ST} = 0.0008$**
Total	226	7.35	100	

Table 3. Gravity models based on landscape variables that limit or promote the gene flow in *Bursera cuneata,* considering between-site and at-site factors at 1,000 to 5,000 m scales. We calculated AIC, ΔAIC values and the percentage of variation explained (PVE). Abbreviations: geographic distance (Geo), tropical dry forest (TDF), temperate forest (TF), agriculture (Agri), ecological niche model (Niche), urban areas (Urban), terrain roughness (Rough), East Aspect (Aspect), and slope (Slope). Combined models: comb1) Geo + TDF + Niche; comb2) Geo + TDF + TF; and comb3) Geo + TDF + TF + Niche + Rough. K number of model parameters. Bold letters denote the best-performing model for each spatial scale.

Scale	1000			2000			3000			4000			5000	
Models	AIC	ΔAIC	PVE	AIC	ΔAIC	PVE	AIC	ΔAIC	PVE	AIC	ΔAIC	PVE	AIC	ΔA
Between-site:														
Geo	-3446.08	60.164	26.92	-3446.08	59.503	28.64	-3446.08	79.058	26.94	-3446.08	72.118	25.69	-3446.08	88
TDF	-3457.57	48.668	26.36	-3457.15	48.434	26.74	-3482.82	42.319	39.86	-3487.04	31.15	40.75	-3505.82	28
TF	-3460.34	45.905	15.57	-3462.23	43.349	16.05	-3465.92	59.217	14.62	-3465.16	53.032	20.7	-3462.72	71
Agri	-3435.05	71.192	1.76	-3436.26	69.322	1.8	-3435.57	89.562	1.91	-3435.51	82.689	5.7	-3435.87	98
Niche	-3437.43	68.815	9.13	-3440.18	65.4	16.64	-3442.65	82.487	10.61	-3437.58	80.61	2.9	-3438.57	95
Urban	-3438.65	67.589	3.35	-3437.87	67.707	3.73	-3436.21	88.927	3.84	-3436.37	81.823	3.1	-3436.7	97
Rough	**-3506.24**	**0**	**46.72**	**-3505.58**	**0**	**45.08**	-3505.72	19.411	43.64	-3499.67	18.521	36.99	-3488.32	46
At-site:														
Aspect	-3436.89	69.346	0.43	-3436.89	68.685	1.7	-3436.89	88.24	0.9	-3436.89	81.3	2.9	-3436.89	97
Slope	-3437.02	69.224	0.68	-3437.02	68.563	1.9	-3437.02	88.118	0.19	-3437.02	81.178	0.59	-3437.02	97
Combined Models:														
Comb1	-3446.83	59.408	24.28	-3448.4	57.184	18.01	-3475.91	49.222	19.31	-3475.66	42.53	11.98	-3495.18	39
Comb2	-3464.88	41.36	35.1	-3467.68	37.901	24.76	-3494.57	30.566	18.21	-3502.28	15.918	11.59	**-3534.38**	**0**
Comb3	-3501.28	4.957	55.54	-3500.83	4.754	37.38	**-3525.13**	**0**	**52.44**	**-3518.19**	**0**	**49.54**	-3524.75	9.6

Figures

Fig 1.

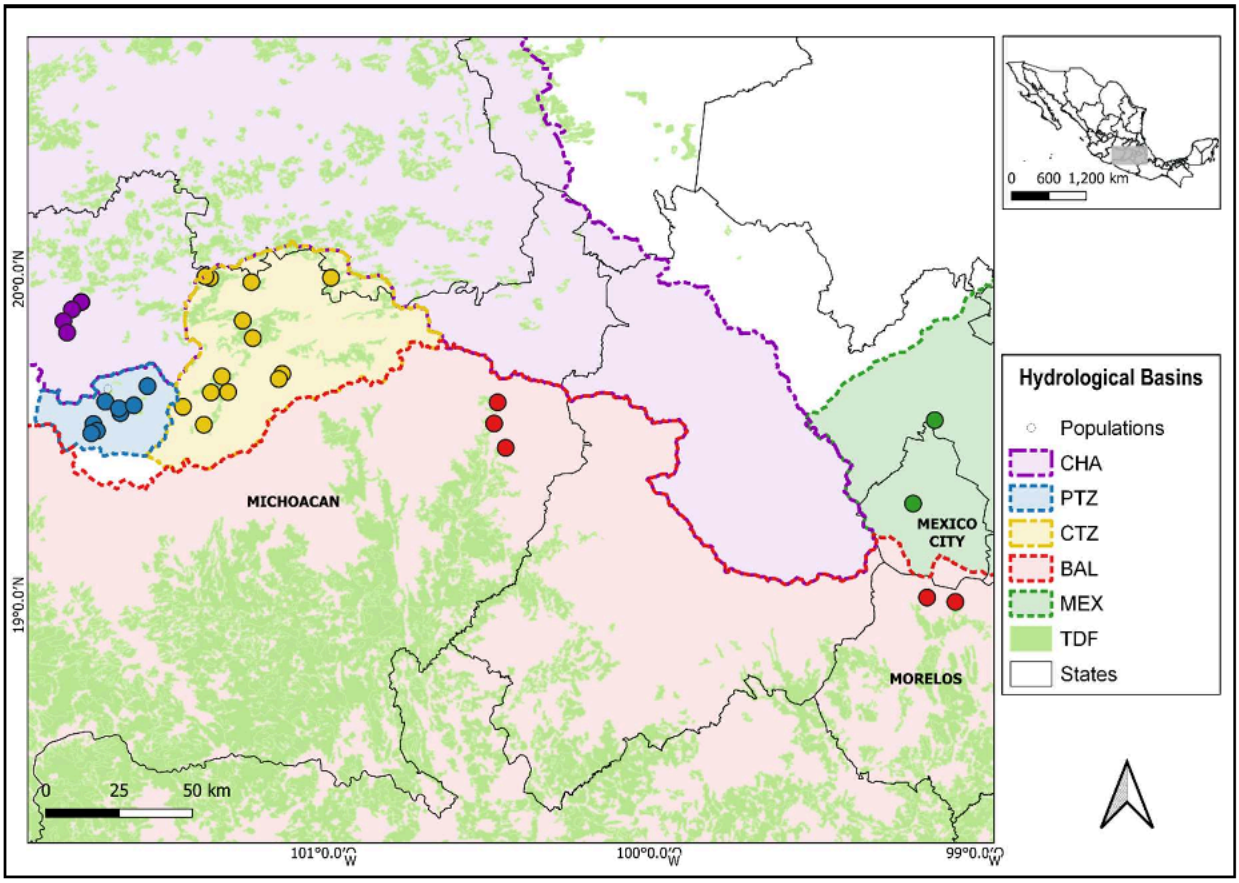

Figure 1

Geographical location of the 33 populations collected for *B. cuneata* covering the states of Michoacán, Mexico City and Morelos. The populations were divided according to the hydrological basins: Lerma-Chapala basin (CHA), Patzcuaro Lake (PTZ), Cuitzeo Lake (CTZ), Balsas River basin (BAL) and Mexico´s basin (MEX).

Fig. 2

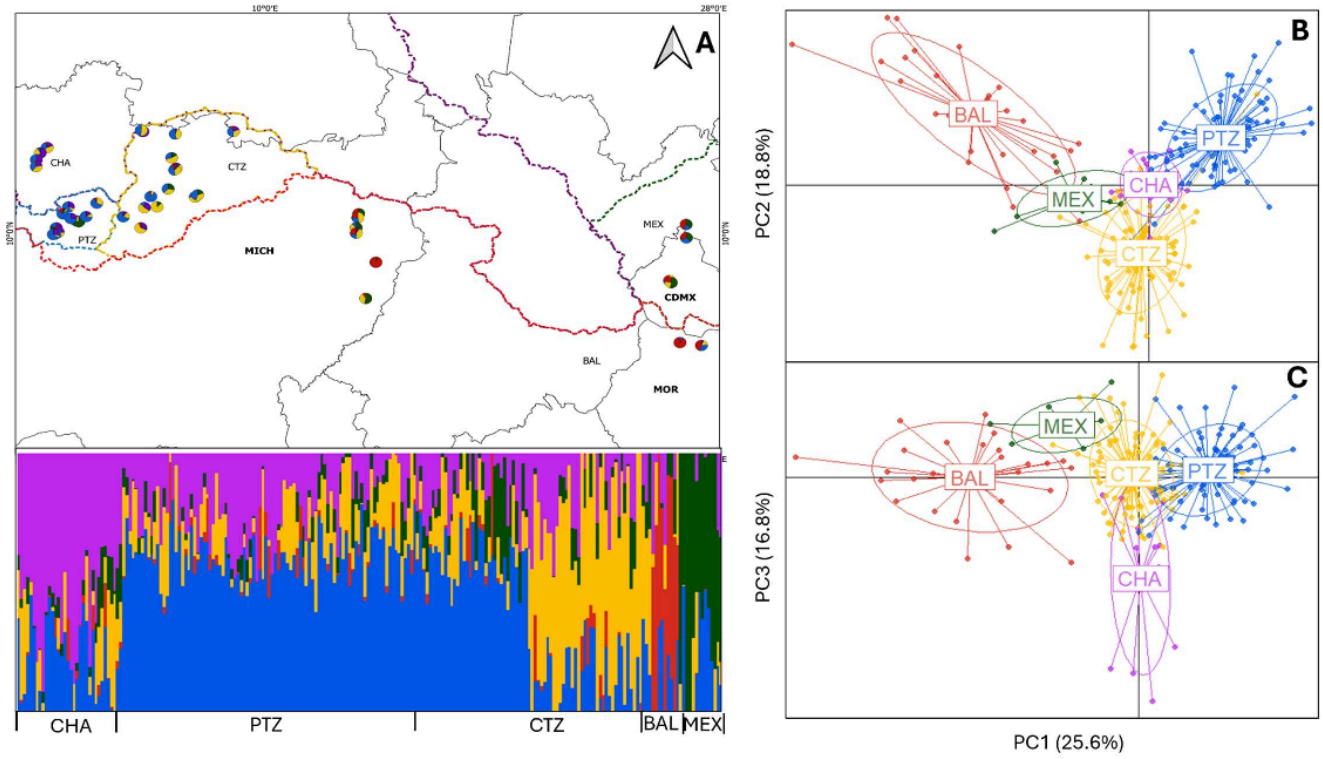

Figure 2

Results from clustering analysis: A. The genetic structure obtained in *LEA* with the best K = 5 is shown using a barplot and pie charts on a map for each sampled population in *Bursera cuneata*, as well as its distribution in the Lerma-Chapala basin (CHA), Patzcuaro Lake (PTZ), Cuitzeo Lake (CTZ), Balsas River basin (BAL) and Mexico´s basin (MEX). B. The DAPC shows differentiation among five hydrological basins (CHA, PTZ, CTZ, BAL, and MEX basins), defined a priori. C. DAPC made from principal components one and three.

Fig. 3

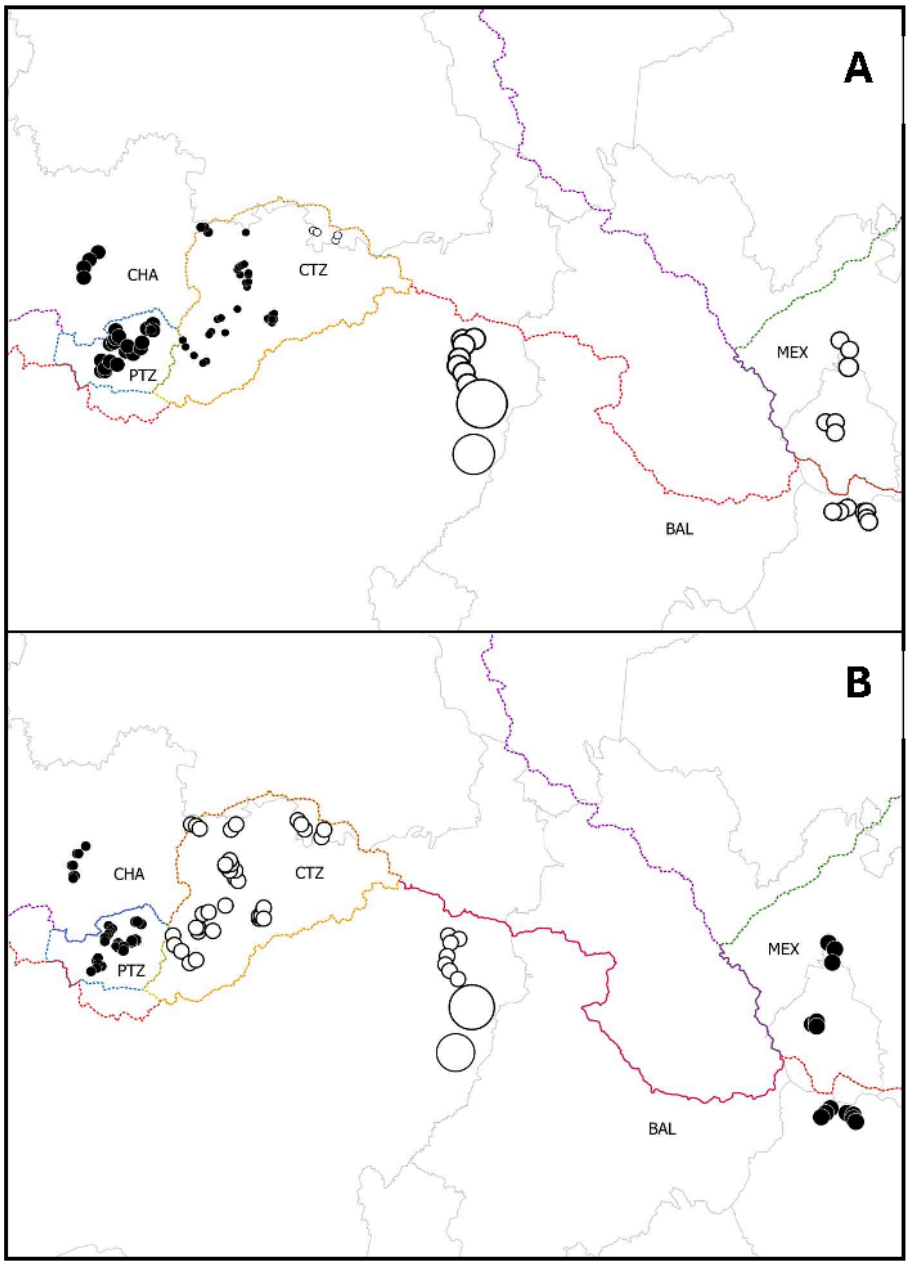

Figure 3

Results from Moran's Eigenvector Maps (MEM). Larger circles represent a greater contribution to the spatial pattern of each eigenvector. A. MEM1 and B. MEM2

Fig. 4

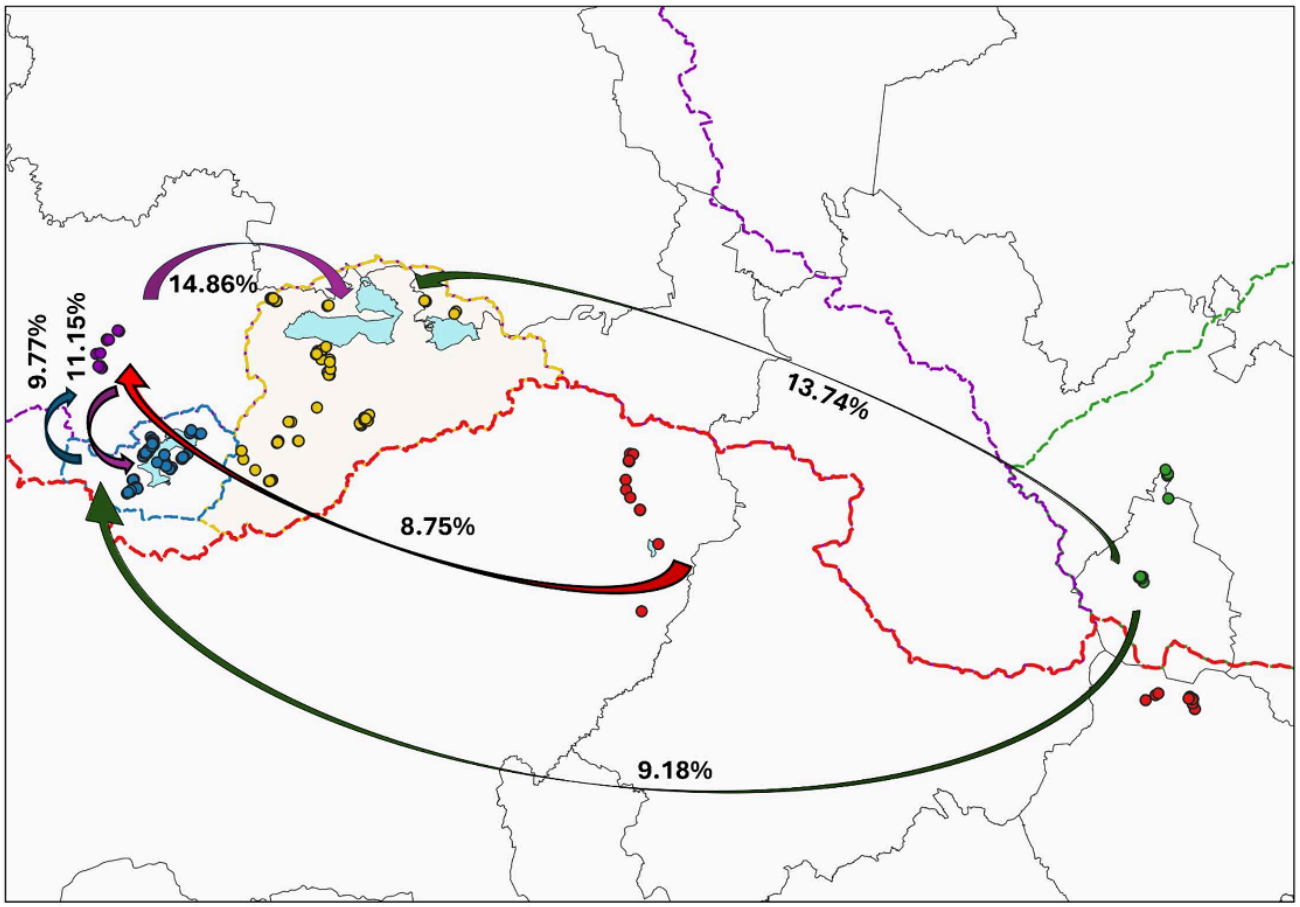

Figure 4

BayesAss analysis results from contemporary migration rates among the Lerma-Chapala basin (CHA), Patzcuaro Lake (PTZ), Cuitzeo Lake (CTZ), Balsas River basin (BAL) and Mexico´s basin (MEX), denoting the main asymmetrical gene flow rates among basins in percentage of migrants.

Supplementary Files

This is a list of supplementary files associated with this preprint. Click to download.

- SupplementalinformationLandscapegenetics.docx